Adsorption and photocatalytic degradation performances of TiO$_2$/diatomite composite for volatile organic compounds: Effects of key parameters

Guangxin Zhang[a,b,c,*], Yangyu Liu[b], Zaher Hashisho[c,*], Zhiming Sun[b,*], Shuilin Zheng[b], Lexuan Zhong[d]

[a] School of Materials Science and Engineering, Shandong University of Science and Technology, Qingdao 266590, PR China
[b] School of Chemical and Environmental Engineering, China University of Mining & Technology (Beijing), Beijing 100083, PR China
[c] Department of Civil and Environmental Engineering, University of Alberta, Edmonton, AB T6G 2W2, Canada
[d] Department of Mechanical Engineering, University of Alberta, Edmonton, AB T6G 1H9, Canada

ABSTRACT

The TiO$_2$/diatomite composites with excellent adsorption and photo-degradation performances were leveraged to investigate the influences of calcination temperature and operating factors on their properties. The results showed that the calcination temperature was closely bound up with the crystallization of TiO$_2$ and the specific surface area of composite. The composite with calcination temperature of 550 °C exhibited enhanced photo-catalytic owing to the high surface area and small TiO$_2$ crystallite size. A series of dynamic degradation experiments were conducted to investigate the effect of various operating parameters on acetone and *p*-xylene adsorption/degradation performances of the composite. The results illustrated that when the relative humidity (0–70%), gas flow rate (1–4 L/min), and VOC concentration (10–40 ppm) were set as the low values, the high total organic carbon degradation rate could be acquired. The total organic carbon degradation rate reached to a high value when the composite dosage was 3.76 mg/cm^2. With the increase of light intensity (0.48–1.33 mW/cm^2), the total organic carbon degradation rate presented an upward trend and then kept stable. The absorbent-photocatalyst hybrid TiO$_2$/diatomite composite could be the promising VOC purification materials.

1. Introduction

Environmental pollution has become a pressing problem, especially for air contamination such as dust pollution, haze, acid rain, etc. Frequent pollution incidents made people aware of the seriousness of air pollution, and also, some air quality indexes are attracting more focuses [1–4]. Rapid urbanization and industrialization have led to the increasing emissions of volatile organic compounds (VOCs). VOCs are diverse, extensive, and complex. Release sources of VOCs are extensive, including automobile exhaust, chemical industry, paper industry, petroleum smelting, and textile industry; while indoor pollution sources mainly come from building materials, furniture, coatings, office supplies, and insulating materials [5,6]. Studies have shown that VOCs can directly or indirectly trigger environmental issues [7]. VOCs are important precursors for urban haze and photochemical smog. The massive VOC emissions led to ozone layer destruction, abnormal weather, sick building syndrome, and other air pollution problems. Exposure in high VOCs concentration environment can cause adverse results for human health, including damage to the respiratory and nervous systems, headache, nausea, and other symptoms, and even cancer [8,9]. It is a common understanding to solve air pollution problems.

Nowadays, how to effectively purify the polluted air is a difficult yet critical issue for researchers. Together with the technologies of solving air pollution problems, various air purification materials are born out. According to VOC species and concentrations, VOC purification treatment methods are also relatively diversified. Commonly, VOC purification methods fall into two categories: recovery and destruction method [10,11]. Among these air purification technologies, physical adsorption, chemical absorption [12], advanced oxidation [13], membrane separation [14], and other joint technologies are the focuses [15]. Of all VOC treatment methods, adsorption is one of the operational, simple and low-cost VOC purification technologies. VOC adsorption technology mainly relies on the large specific surface area and pore volume of the adsorption material to fix VOC molecules. Therefore, for the adsorption process, the key point is to identify the adsorbent with high adsorption capacity and excellent adsorption efficiency. However, the adsorption of VOC by porous materials is mostly a physical adsorption process, which is prone to secondary pollution after

saturation. If porous materials are endowed with catalytic ability, VOC molecules after adsorption can be gradually degraded into non-toxic and harmless molecules, and then the sustainability of air purification can be realized. There are many studies on photocatalysis, mainly focusing on the basic principle of photo-degradation, enhancing the efficiency of photocatalyst, and expanding the application fields of photocatalysis [16,17]. The core part of this technology is the construction of photocatalytic materials.

Mineral resources have enormous reserves on the earth. How to implement them in air purification is a popular research area in the field of mineral materials and environmental engineering. Porous minerals have special pore structure and outstanding adsorption performance, which can provide special physicochemical adsorption or microchemical reaction sites. The principal components of these minerals are silicon endowed with stable structure and chemical properties. Adsorbent-photocatalyst hybrid materials have been widely used for enhancing the photocatalytic performance of photocatalysts [18]. Natural porous minerals that have excellent adsorption and capture functions are often been utilized as the adsorption carries [19]. Supporting TiO$_2$ nanoparticles on the surface of non-metallic minerals is not only conducive to inhibit the growth of TiO$_2$ grains but also conducive to the recovery and utilization of photocatalysts. In the past few years, some inherent non-metallic minerals had been used as supporting minerals for TiO$_2$ [20–24]. Diatomite is a biogenic siliceous sedimentary rock composed of diatoms skeletal remains. The main phase of diatomite is amorphous silicon dioxide. There has many regular large pores arranged symmetrically on the surface of diatomite. The porous structure, stable chemical properties, and abundant reserves make it used extensively as adsorbents and catalyst supports. The preparation and photocatalytic activities of these composites have been reported by many literatures. However, there is lack of the researches about the impacts of operating factors on the VOC purification performances of these adsorbent-photocatalyst hybrid materials.

In view of this, this paper mainly detailed the VOC adsorption and photocatalytic degradation performances of TiO$_2$/diatomite composites. With formaldehyde, acetone, and p-xylene as the pollutants, the effects of calcination temperature and operating parameters (relative humidity, VOC concentration, gas flow rate, catalyst dosage, and light intensity) on adsorption/photo-degradation performances were investigated.

2. Experimental

2.1. Materials

The TiO$_2$/diatomite composite was used as a photocatalyst in this work. The preparation and characterization methods of this composite followed a reported procedure [25]. The dried samples after hydrolytic precipitation were calcined at different temperatures for 2 h in an electric muffle furnace (in air, heating rate of 5 ℃/min). The composite calcinated at 450 ℃, 550 ℃, 650 ℃, 750 ℃, and 850 ℃ were labeled as TD-X (X means the calcination temperature). Formaldehyde, acetone, and p-xylene were treated as the model VOC pollutants. The chemical structures of VOCs are illustrated in Fig. 1.

2.2. Adsorption and photocatalytic degradation experiments

The adsorption and photocatalytic degradation experiments for formaldehyde were evaluated by a photoreactor as described in the literature [25]. Typically, a glass plate with 1.0 g of the composite was placed in a formaldehyde environment and irradiated by UVA lamps (8 W, 365 nm) at a relative humidity of 60%. The dark and illumination time was 120 min and 90 min, respectively. The concentration of formaldehyde was evaluated according to the spectrophotometric method. Experiments for acetone and p-xylene were evaluated by a continuous stream device. The experimental setup is shown in Fig. 2. The VOC gas
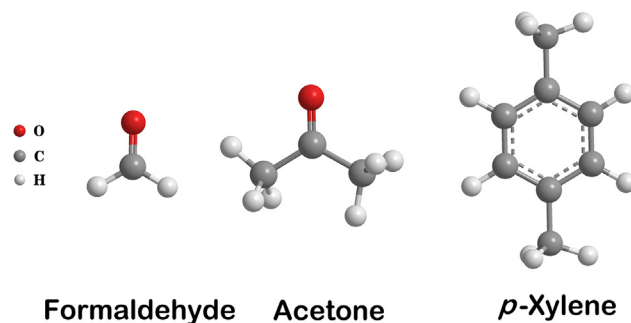

Fig. 1. Chemical structures of formaldehyde, acetone, and p-xylene.

was generated by injecting the liquid acetone or p-xylene into the air stream using a syringe pump. The relative humidity of the experiment was controlled by adjusting the flow rate of wet air and dry air. Powder sample mixing with water was dispersed by ultrasonic and the slurry was coated on an aluminum substrate. The aluminum substrate was put in the reactor and sealed by the quartz plate. The reactor (0.13 L) was illuminated by UVA lamps. The initial experimental conditions were set as following: relative humidity (RH) is closed to 0% (dry compressed air), VOC concentration is 10 ppm, catalyst dosage is 2.26 mg/cm^2, gas flow rate is 1 L/min, and light intensity is 0.78 mW/cm^2. The total organic carbon concentration was tested by a total hydrocarbon analyzer (Series 9000, Baseline Mocon).

3. Results and discussion

3.1. Effect of calcination temperature

The XRD patterns of TiO$_2$/diatomite composites are shown in Fig. 3(a). The TiO$_2$/diatomite composites exhibited peaks corresponding to anatase (JCPDS 21-1272). Starting from 450 ℃, with the increase of temperature, TiO$_2$ gradually changed from amorphous to anatase. When the calcining temperature is 450 ℃, although the characteristic peak of anatase TiO$_2$ has appeared, the peak intensity is weak. It indicated that the TiO$_2$ was changing from amorphous to anatase, but the crystallinity of anatase TiO$_2$ is not high. When the crystallinity of TiO$_2$ is low, there are more defects in the body phase. The defects will become the description center of photogenerated electrons and holes, which is not conducive to the photocatalytic reaction. When the calcining temperature is 550 ℃, anatase TiO$_2$ was formed with relatively complete crystallization, and the complete crystal structure is beneficial to the process of photocatalytic reaction. With the gradual increase of calcining temperature, the characteristic peaks of anatase TiO$_2$ became more and more obvious, indicating that the crystallinity of nano TiO$_2$ was getting better and better, and the grain size of TiO$_2$ was getting larger and larger. When calcination temperature reached 850 ℃, part of anatase had transformed into the rutile phase. According to the Scherrer equation, the average crystallite sizes of TiO$_2$ in TiO$_2$/diatomite composites were calculated and listed in Table 1. The crystallite size of TiO$_2$ became larger with the rise of calcination temperature. This may be due to the high frequency of aggregation and sintering among the TiO$_2$ nanoparticles. Generally, a smaller crystallite size is beneficial to the photocatalytic activity.

N$_2$ adsorption-desorption was carried out to examine the porous structures TiO$_2$/diatomite composites. Fig. 3(b) and Fig. 3(c) shows the N$_2$ adsorption-desorption isotherms and the BJH pore size distributions of diatomite and TiO$_2$/diatomite. As expected, the N$_2$ volume adsorbed by TiO$_2$/diatomite composite dropped as the calcination temperature climbed, which may be explained by the fact that the crystallite size of TiO$_2$ increased with the calcination temperature and also the mesoporous structure of the diatomite may be damaged under high calcination temperature. It can be seen from Table 1 that TD-450 showed
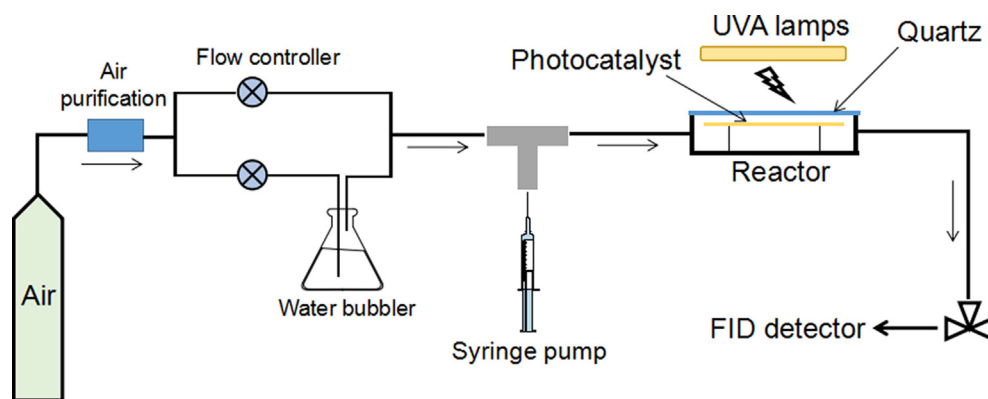
Fig. 2. Schematic diagram of adsorption and photocatalytic degradation setup.

higher values of surface area and pore volume. As shown in Fig. 3(b), the isotherms of TiO₂/diatomite composites calcined at 450–650 °C were identified as type IV with an H3 hysteresis loop, which was the characteristic of mesoporous materials. Probably, the mesoporous structure was thought to result from the deposition and aggregation of TiO₂ nanoparticles on the surface of diatomite. Using the BJH method and desorption branches of the isotherms, the pore size distributions of TiO₂/diatomite fall into the range of 2 to 15 nm (Fig. 3c). The specific surface area and pore structure parameters of the TiO₂/diatomite composites are listed in Table 1. It can be seen that the TD-450 presented the maximum specific surface area (52.2 m²/g) and pore volume (0.082 cm³/g). The specific surface area and pore volume of TiO₂/diatomite composites showed a downward trend with the ascending calcination temperature.

Fig. 3(d-f) presents the adsorption and photocatalytic activity of TiO₂/diatomite composites with different calcination temperatures for formaldehyde and acetone under UV light irradiation. It is worth to remark that the adsorption capacities of these composites declined with the increasing calcination temperature. This is because that the TiO₂/diatomite composites prepared under low calcination temperatures had higher surface area and pore volume. As for the acetone adsorption

Table 1
TiO₂ crystallite sizes, surface area, and pore volume of TiO₂/diatomite composites.

Sample	TiO₂ crystallite size (nm)	BET specific surface area (m²/g)	Pore volume (cm³/g)
TD-450	8.9	52.2	0.082
TD-550	10.9	40.0	0.078
TD-650	14.2	25.6	0.053
TD-750	26.8	16.5	0.029
TD-850	29.2	10.3	0.019

breakthrough curves, the composite with high surface area and pore volume had the long adsorption time indicating the high adsorption capacity. Surprisingly, TD-450 with the highest adsorption capacity showed a rather poor photo-activity for the degradation of formaldehyde and acetone. This may be due to the weak crystallinity of TiO₂ in TD-450. The low crystallization indicated more existing crystal structure defects in TiO₂, which resulted in the rapid recombination of photo-induced electrons and holes. TD-550 had a higher degradation efficiency for both formaldehyde and acetone, which was attributed to
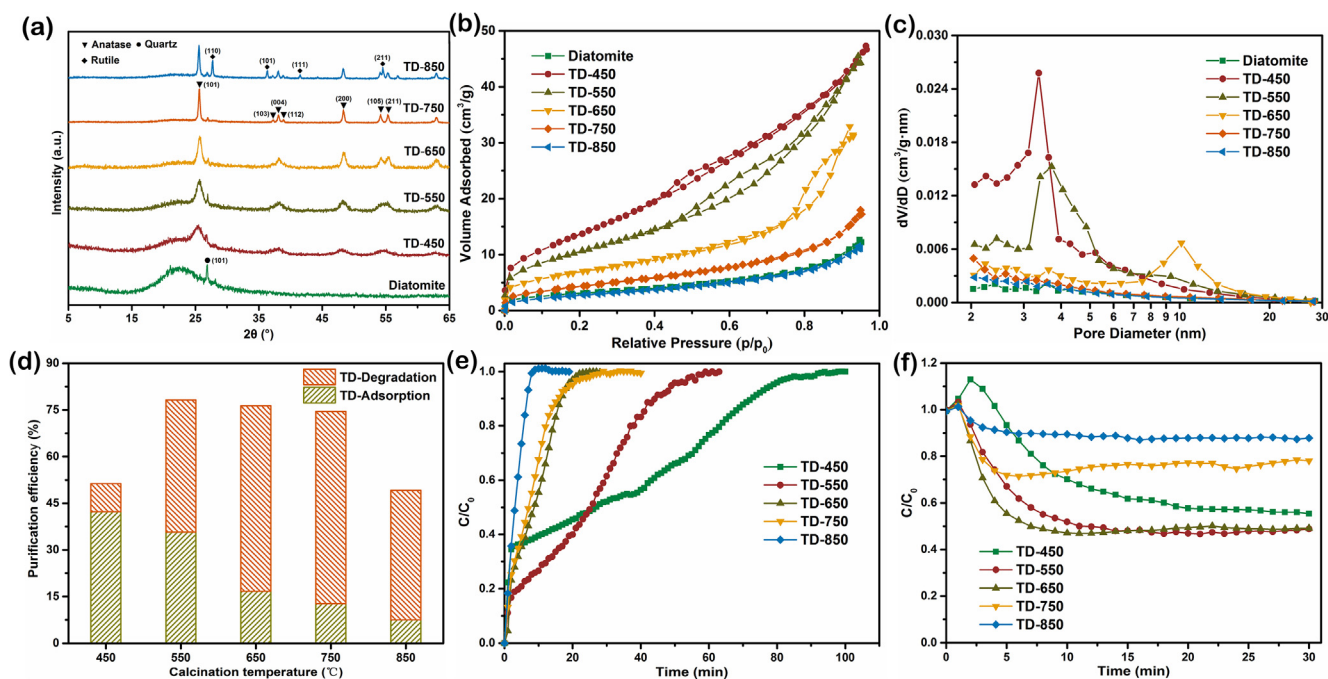

Fig. 3. (a) XRD patterns, (b) N₂ adsorption-desorption isotherms, (c) pore size distributions, (d) formaldehyde adsorption-degradation, and (e, f) acetone adsorption and degradation of TiO₂/diatomite.

its higher adsorption capacity and TiO$_2$ crystallization. The strong adsorption performance provided more access to the photocatalytic active sites of TiO$_2$. The improved crystallization of TiO$_2$ enhanced the separation efficiency of the photo-generated electrons and holes because of the decrease of recombination center in bulk TiO$_2$ [26–28]. Therefore, more radicals can be produced and reacted with formaldehyde and acetone. However, with the rising calcination temperature up to 650 °C and more, the surface area and pore volume of TiO$_2$/diatomite declined as well as the crystallite size of TiO$_2$ increased. These trends gave rise to the low adsorption capacity and photocatalytic activity of TiO$_2$/diatomite. The results and analysis indicated that the coexistence of high surface area and small crystallite size of TiO$_2$ was required for obtaining optimum photocatalytic performance.

3.2. Effect of operating parameter

In this series of experiments, acetone (polar VOC) and *p*-xylene (non-polar VOC) were used as pollutants. Relative humidity, VOC concentration, gas flow rate, catalyst dosage, and light intensity were regarded as operating parameters. The composite TD-550 was used as the photocatalyst. For the relative humidity experiment, the RH was set as 0%, 15%, 30%, 50%, and 70%. The relative humidity experimental results are presented in Fig. 4. The relative humidity had a significant effect on the adsorption properties of *p*-xylene on composites. When RH = 0%, the adsorption saturation time for *p*-xylene was the longest. The adsorption saturation time was sharply reduced when the relative humidity rose to 15%. With the gradual rising of relative humidity, the adsorption saturation time of composite for *p*-xylene was gradually declined. The amounts of *p*-xylene adsorbed by the composite under different relative humidity reduced as the relative humidity gradually increased. The effect of relative humidity on adsorption performance was mainly due to the competitive adsorption of water molecules and VOC molecules on the surface of the composite. When VOC gas with certain humidity was introduced into the reactor, the water molecules were more likely to be adsorbed on the surface of the composite. When the water molecules occupied the adsorption sites over the surface of the composite, the VOC molecules could no longer be adsorbed by the composite and only be discharged out of the reactor along with the gas. When the adsorption of the composite for VOC was saturated, the ultraviolet light was turned on, and the VOC gas began to be degraded. Fig. 4(b) shows the variation curves of total organic carbon (TOC) concentration during the photocatalytic degradation process. It can be observed that after the start of the lighting, the TOC content at the outlet of the reactor dropped rapidly, and after a period of time, it tended to be stable. The TOC concentration changes were different under different RH. When RH = 0%, the TOC concentration descended around 60%. As relative humidity grew, the TOC concentration changes

were reduced. The average TOC degradation rate (after 20–30 min of illumination) decreased from 63.4% to 12.2% as the RH rose from 0% to 70%. The above analysis showed that the adsorption and photocatalytic degradation performances of the composite were susceptible to RH [29,30].

For the gas flow rate experiment, the gas flow rate was set as 1, 2, 3, and 4 L/min. The experimental results are shown in Fig. 5. The adsorption saturation time of the composite decreased gradually with the increase of flow rates. For acetone, the adsorption saturation time dropped from 60 min to 20 min as the gas flow rate increased from 1 L/min to 4 L/min. Depending on the above analysis, the effect of gas flow rate on adsorption performance was mainly reflected by the fact that the gas flow rate determined the amount of adsorbed VOC molecules and the residence time of VOC molecules on the composite surface. When a certain amount of VOC gas was introduced into the reactor, the number of VOC molecules entering the reactor per unit time was determined. The larger the flow rate, the more the VOC molecules introduced per unit time, and the more favorable the acetone molecules were adsorbed on the surface of the material. However, the residence time of the VOC molecules on the surface of the composite was shortened when the gas flow rate rose high enough [31,32]. Therefore, the VOC molecules that were not adsorbed by the composite were taken out by the subsequent acetone gas, inducing that the situation of low acetone adsorption amount of composite. For the degradation curves of composites under different gas flow rates, as the gas flow rate increase, the TOC concentration changed differently. The average TOC degradation rate was 52.5% (acetone) and 66.0% (*p*-xylene) when the gas flow rate was 1 L/min. As the gas flow rate increased to 4 L/min, the degradation rate dropped to 14.2% (acetone) and 29.2% (*p*-xylene). The above analysis showed that the low gas passing rate facilitated the process of VOC photocatalytic degradation. Furthermore, the residence time of VOC molecules on the catalyst surface was the determinant of the photocatalytic process. The long residence time was conducive to the complete degradation and the high degradation efficiency of VOC [31,32], which may be helpful for producing less intermediate products. Generally, the mass transfer rate of pollutants increased with the increase of flow rates. With the rising flow rate, the gas residence time became shorter. As a result, the generated intermediate products could not be decomposed timely and the catalyst surface was covered by VOC molecules, leading to the reduction of degradation rate.

For the VOC concentration experiment, the VOC concentration was set as 10, 20, 30, and 40 ppm. The experimental results are shown in Fig. 6. The adsorption saturation time of the composite decreased gradually as the VOC concentration grew. The effect of VOC concentration on adsorption performance was mainly reflected in that the VOC concentration determined the amount of VOC molecules entering the reactor per unit time. The high VOC concentration rendered more
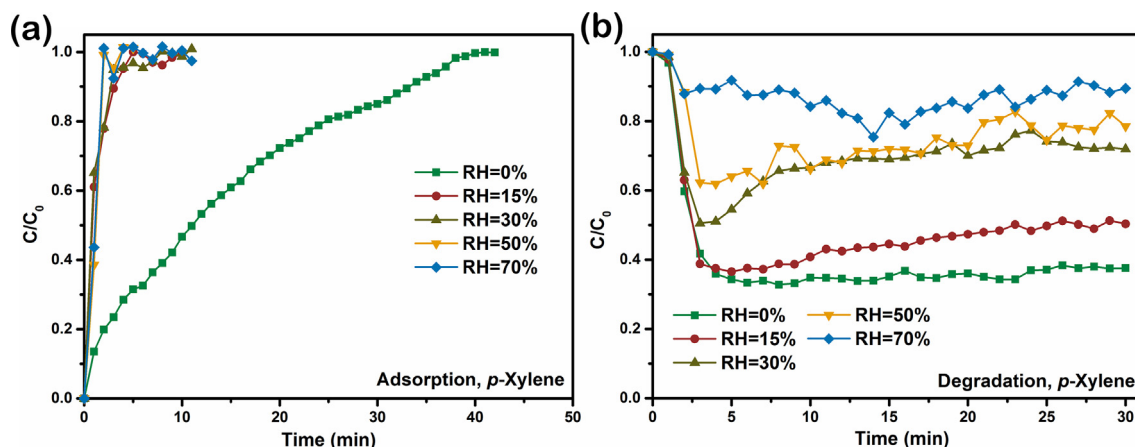

Fig. 4. Adsorption and photocatalytic degradation performances of TiO$_2$/diatomite (TD-550) for *p*-xylene under different relative humidity.
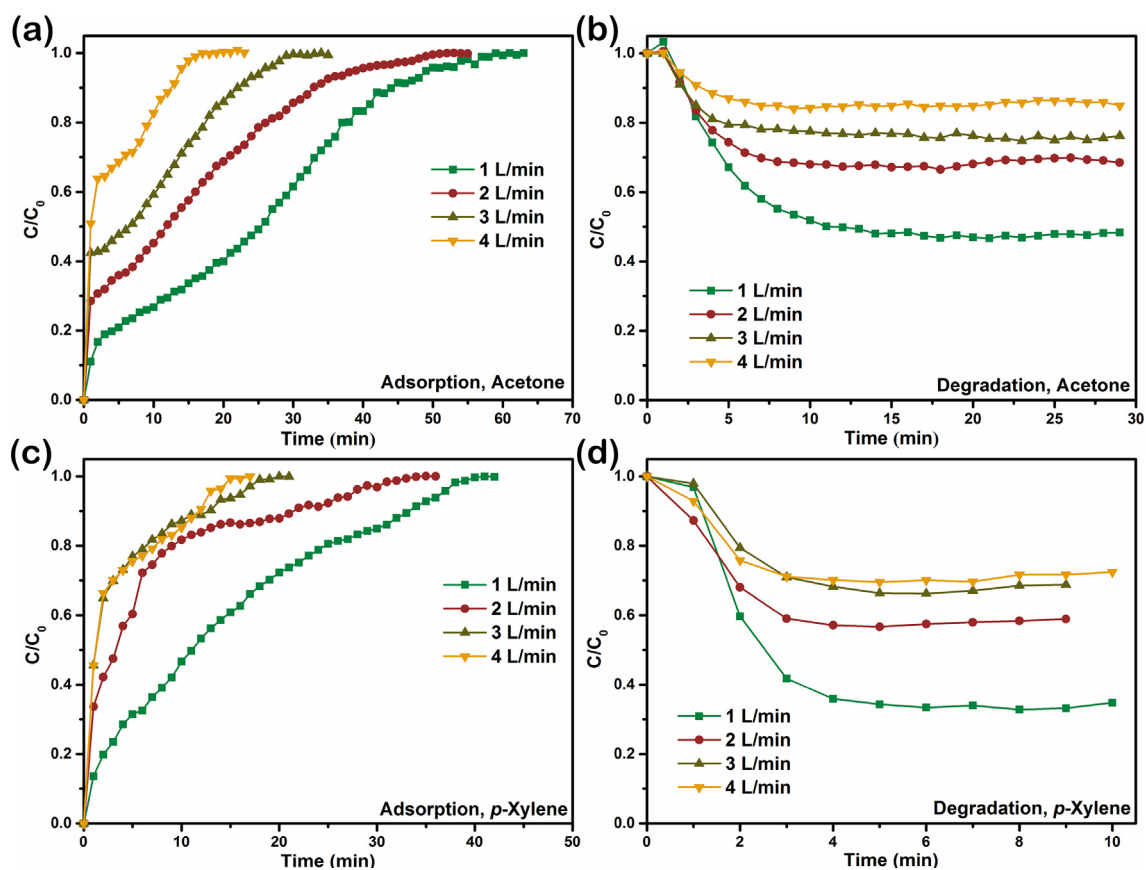
Fig. 5. Adsorption and photocatalytic degradation performances of TiO$_2$/diatomite (TD-550) for acetone and *p*-xylene under different flow rates.

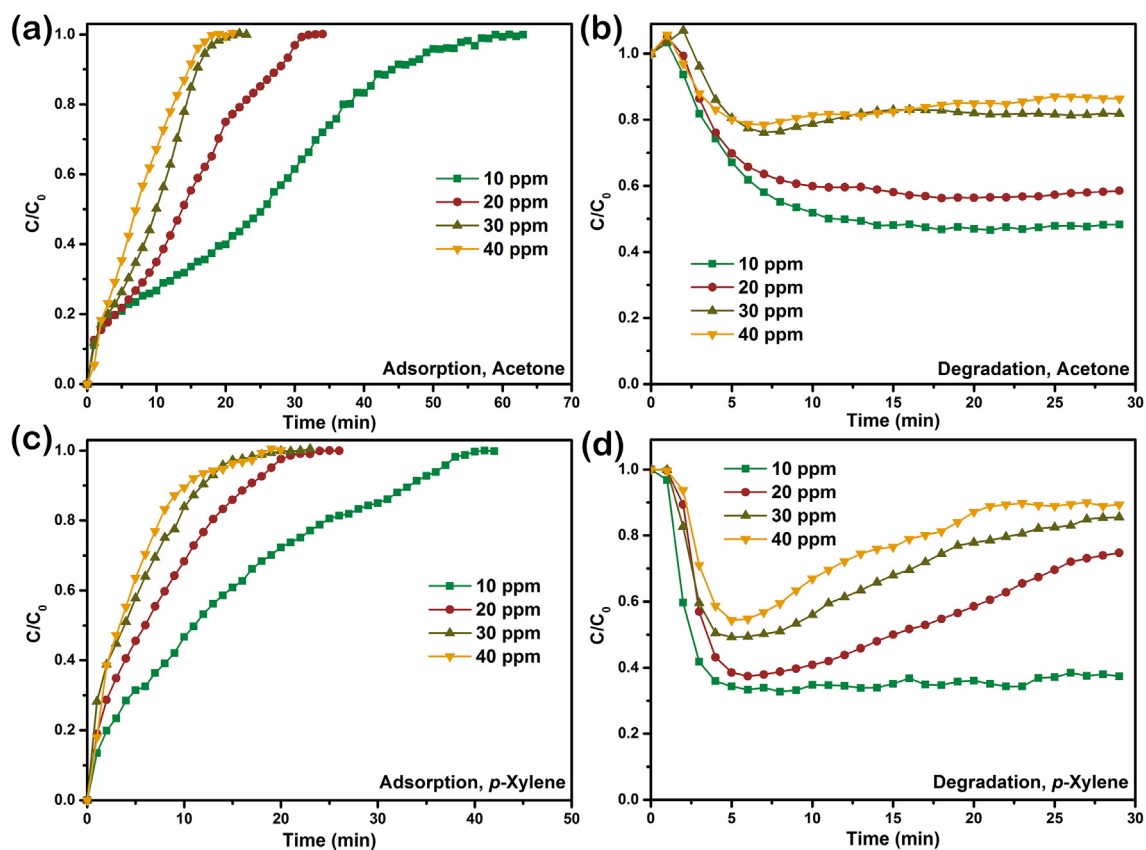**Fig. 6.** Adsorption and photocatalytic degradation performances of TiO$_2$/diatomite (TD-550) for acetone and *p*-xylene under different VOC concentrations.

VOC molecules entering the reactor, resulting in VOC molecules were capable of contacting the catalyst to facilitate the adsorption of more VOC molecules by the catalyst. For the degradation curves of composites under different VOC concentrations, when the VOC concentration was 10 ppm, the degradation rate of the composite was 52.5% (acetone) and 63.5% (p-xylene). The degradation rate decreased gradually to 14.1% (acetone) and 10.9% (p-xylene) as the VOC concentration grew to 40 ppm. The difference trend of degradation curves between acetone and p-xylene may be related to their structures. p-Xylene has more complex structure than acetone inducing the difficult of degradation. The p-xylene and intermediate products were adsorbed by the composite, which resulted in the poisoning of photocatalyst. Therefore, the degradation curves of p-xylene had the increasing trend after illuminating for a while, which means the decreased degradation rate of p-xylene. The above test results showed that the low VOC concentration was a benefit for photocatalytic degradation. The high VOC concentration resulted in more VOC molecules were adsorbed on the surface of the composite. Although the certain gas purging was existing, the acetone concentration was maintained at a higher concentration in the reactor, which was not conducive to the removal of the photocatalytic products, and not helpful for the photocatalytic degradation process of VOC molecules. The VOC had a high consumption rate for free radicals under the high VOC concentration. As the VOC concentration increased, the catalyst surface active point was partially or completely covered by VOC molecules and degradation intermediates, which resulted in the deactivation of the photocatalyst and the reduction of degradation rate [33].

For the catalyst dosage experiment, the catalyst dosage was set as 0.75, 2.26, 3.76, and 5.26 mg/cm^2. The experimental results are shown in Fig. 7. The total adsorption amount of acetone under the condition of different catalyst dosages increased with a rise of catalyst amount. Fig. 7(b) is the curves of total organic carbon in the photocatalytic degradation of composites. As the amount of catalyst increased from 0.75 mg/cm^2 to 2.26 mg/cm^2, the total organic carbon degradation rate increased subsequently. During the increasing process of catalyst amount from 2.26 mg/cm^2 to 5.26 mg/cm^2, the total organic carbon degradation curve changed obviously. When the lamp was activated, the total organic carbon concentration of catalyst dosage of 5.26 mg/cm^2 decreased slowly. The amount of acetone adsorbed by the photocatalyst during the adsorption process was large enough under the high level of catalyst dosage. Under irradiation, the acetone adsorbed on the surface of the composite was degraded firstly. Because of the large amount of acetone adsorbed at this moment, more time was required for the degradation process. The acetone molecules were gradually degraded with the continuous illumination, then the dynamic degradation equilibrium was reached, and the degradation rate of total organic carbon tended to be stable. However, under the condition of high catalyst amount, the adsorbed acetone molecules occupied the surface-active sites of composite, which was not conducive to the desorption and degradation of photocatalytic intermediates, hence impeded the degradation process.

For the light intensity experiment, the light intensity was adjusted to 0.48, 0.78, and 1.33 mW/cm^2. The test results are shown in Fig. 7(c), which shows variation curves of total organic carbon under different UV light intensities. When the light intensity was 0.48 mW/cm^2, the total organic carbon degradation rate was 25.8%. As the light intensity increased to 0.78 mW/cm^2 the total organic carbon degradation rate increased by two times to 52.5%. After continuing to enhance the light intensity to 1.33 mW/cm^2, the total organic carbon degradation rate had hardly changed. This is because, to some extent, increasing the light intensity enables more TiO_2 to be excited, resulting in more hydroxyl radicals and thereby increasing the degradation rate of total organic carbon. However, when the TiO_2 has already been excited, the increase of light intensity has no impact on the degradation rate obviously.

4. Conclusions

The calcination temperature was a key parameter that determined the crystallite size and phase of TiO_2 nanoparticles. The surface area and pore volume of TiO_2/diatomite composite displayed a downtrend with the increase of calcination temperature. TD-550 had a high formaldehyde and acetone degradation rate due to its excellent adsorption performance and crystallinity of TiO_2. The operating parameters, including relative humidity, VOC concentration, and gas flow rate, had significant effects on the adsorption and photo-degradation performances of the acetone and p-xylene over composite. In the process of testing the operating parameters, the higher the relative humidity was, the smaller the adsorption amount owing to the competitive adsorption of VOC and water and the worse the degradation of VOC on composite. The high gas flow rate induced short VOC residence time on the composite surface, leading to the low TOC degradation rate. The high VOC concentration contributed to the high adsorption capacity and the low total organic carbon degradation rate of the composite. The catalyst dosage and light intensity also had an obvious influence on the adsorption and photocatalytic degradation performances of the composite. Overall, this work has practical implications for the application of TiO_2/diatomite composite.

CRediT authorship contribution statement

Guangxin Zhang: Conceptualization, Methodology, Investigation, Writing - original draft, Formal analysis, Software. **Yangyu Liu:** Investigation. **Zaher Hashisho:** Writing - review & editing, Supervision. **Zhiming Sun:** Writing - review & editing. **Shuilin Zheng:** Supervision. **Lexuan Zhong:** Writing - review & editing.

Declaration of Competing Interest

The authors declare that they have no known competing financial interests or personal relationships that could have appeared to
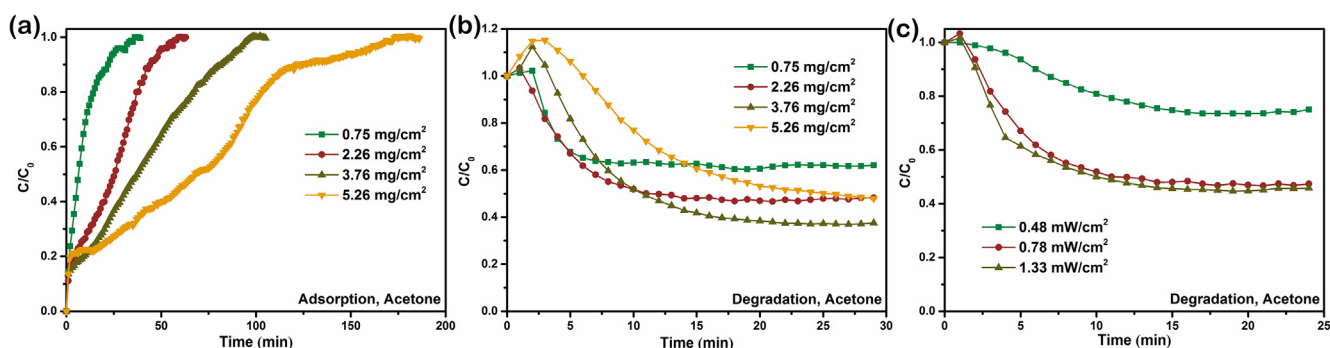

Fig. 7. Adsorption and photocatalytic degradation performances of TiO_2/diatomite (TD-550) for acetone under different catalyst dosage and UV intensity.

influence the work reported in this paper.

References

[1] C. Song, L. Wu, Y. Xie, J. He, X. Chen, T. Wang, Y. Lin, T. Jin, A. Wang, Y. Liu, Q. Dai, B. Liu, Y.-N. Wang, H. Mao, Air pollution in China: status and spatio-temporal variations, Environ. Pollut. 227 (2017) 334–347.

[2] R. Zhang, C. Liu, P.-C. Hsu, C. Zhang, N. Liu, J. Zhang, H.R. Lee, Y. Lu, Y. Qiu, S. Chu, Y. Cui, Nanofiber air filters with high-temperature stability for efficient PM$_{2.5}$ removal from the pollution sources, Nano Lett. 16 (2016) 3642–3649.

[3] S. Feng, D. Gao, F. Liao, F. Zhou, X. Wang, The health effects of ambient PM$_{2.5}$ and potential mechanisms, Ecotoxicol. Environ. Saf. 128 (2016) 67–74.

[4] C. Song, J. He, L. Wu, T. Jin, X. Chen, R. Li, P. Ren, L. Zhang, H. Mao, Health burden attributable to ambient PM$_{2.5}$ in China, Environ. Pollut. 223 (2017) 575–586.

[5] L. Wang, B. Zhao, C. Liu, H. Lin, X. Yang, Y. Zhang, Indoor SVOC pollution in China: a review, Chin. Sci. Bull. 55 (2010) 1469–1478.

[6] H. Tao, Y. Fan, X. Li, Z. Zhang, W. Hou, Investigation of formaldehyde and TVOC in underground malls in Xi'an, China: concentrations, sources, and affecting factors, Build. Environ. 85 (2015) 85–93.

[7] Y. Ling, Y. Wang, J. Duan, X. Xie, Y. Liu, Y. Peng, L. Qiao, T. Cheng, S. Lou, H. Wang, X. Li, X. Xing, Long-term aerosol size distributions and the potential role of volatile organic compounds (VOCs) in new particle formation events in Shanghai, Atmos. Environ. 202 (2019) 345–356.

[8] Y. Gong, Y. Wei, J. Cheng, T. Jiang, L. Chen, B. Xu, Health risk assessment and personal exposure to Volatile organic compounds (VOCs) in metro carriages – a case study in Shanghai, China, Sci. Total Environ. 574 (2017) 1432–1438.

[9] F. Davardoost, D. Kahforoushan, Health risk assessment of VOC emissions in laboratory rooms via a modeling approach, Environ. Sci. Pollut. Res. 25 (2018) 17890–17900.

[10] M. Słomińska, S. Król, J. Namieśnik, Removal of BTEX compounds from waste gases; destruction and recovery techniques, Crit. Rev. Environ. Sci. Technol. 43 (2013) 1417–1445.

[11] M.S. Kamal, S.A. Razzak, M.M. Hossain, Catalytic oxidation of volatile organic compounds (VOCs) – a review, Atmos. Environ. 140 (2016) 117–134.

[12] L. Li, S. Liu, J. Liu, Surface modification of coconut shell based activated carbon for the improvement of hydrophobic VOC removal, J. Hazard. Mater. 192 (2011) 683–690.

[13] M. Mao, H. Lv, Y. Li, Y. Yang, M. Zeng, N. Li, X. Zhao, Metal support interaction in Pt nanoparticles partially confined in the mesopores of microsized mesoporous CeO$_2$ for highly efficient purification of volatile organic compounds, ACS Catal. 6 (2016) 418–427.

[14] S. Ragunath, S. Mitra, Carbon nanotube immobilized composite hollow fiber membranes for extraction of volatile organics from air, J. Phys. Chem. C 119 (2015) 13231–13237.

[15] A. Luengas, A. Barona, C. Hort, G. Gallastegui, V. Platel, A. Elias, A review of indoor air treatment technologies, Rev. Environ. Sci. Bio/Technol. 14 (2015) 499–522.

[16] Z. Shayegan, C.-S. Lee, F. Haghighat, TiO$_2$ photocatalyst for removal of volatile organic compounds in gas phase – a review, Chem. Eng. J. 334 (2018) 2408–2439.

[17] K. Nakata, A. Fujishima, TiO$_2$ photocatalysis: design and applications, J. Photochem. Photobiol. C-Photochem. Rev. 13 (2012) 169–189.

[18] W. Zou, B. Gao, Y.S. Ok, L. Dong, Integrated adsorption and photocatalytic degradation of volatile organic compounds (VOCs) using carbon-based nanocomposites: a critical review, Chemosphere 218 (2019) 845–859.

[19] G. Zhang, Y. Liu, S. Zheng, Z. Hashisho, Adsorption of volatile organic compounds onto natural porous minerals, J. Hazard. Mater. 364 (2019) 317–324.

[20] G. Zhang, A. Song, Y. Duan, S. Zheng, Enhanced photocatalytic activity of TiO$_2$/zeolite composite for abatement of pollutants, Micropor. Mesopor. Mater. 255 (2018) 61–68.

[21] X. Hu, Z. Sun, J. Song, G. Zhang, S. Zheng, Facile synthesis of nano-TiO$_2$/stellerite composite with efficient photocatalytic degradation of phenol, Adv. Powder Technol. 29 (2018) 1644–1654.

[22] V. Belessi, D. Lambropoulou, I. Konstantinou, A. Katsoulidis, P. Pomonis, D. Petridis, T. Albanis, Structure and photocatalytic performance of TiO$_2$/clay nanocomposites for the degradation of dimethachlor, Appl. Catal. B-Environ. 73 (2007) 292–299.

[23] B. Szczepanik, Photocatalytic degradation of organic contaminants over clay-TiO$_2$ nanocomposites: a review, Appl. Clay Sci. 141 (2017) 227–239.

[24] D. Kibanova, M. Sleiman, J. Cervini-Silva, H. Destaillats, Adsorption and photocatalytic oxidation of formaldehyde on a clay-TiO$_2$ composite, J. Hazard. Mater. 211–212 (2012) 233–239.

[25] G. Zhang, Z. Sun, Y. Duan, R. Ma, S. Zheng, Synthesis of nano-TiO$_2$/diatomite composite and its photocatalytic degradation of gaseous formaldehyde, Appl. Surf. Sci. 412 (2017) 105–112.

[26] J. Li, Y. Wang, Y. Tian, X. He, P. Yang, M. Yuan, Y. Cao, J. Lyu, Crystallization of microporous TiO$_2$ through photochemical deposition of Pt for photocatalytic degradation of volatile organic compounds, Environ. Sci. Pollut. Res. 25 (2018) 15662–15670.

[27] A. Di Bellardita, B. Paola, L. Megna, Palmisano, Determination of the crystallinity of TiO$_2$ photocatalysts, J. Photochem. Photobiol. A 367 (2018) 312–320.

[28] L. Gao, Q. Zhang, Effects of amorphous contents and particle size on the photocatalytic properties of TiO$_2$ nanoparticles, Scr. Mater. 44 (2001) 1195–1198.

[29] E.J. Park, H.O. Seo, Y.D. Kim, Influence of humidity on the removal of volatile organic compounds using solid surfaces, Catal. Today 295 (2017) 3–13.

[30] J. Mo, Y. Zhang, Q. Xu, Effect of water vapor on the by-products and decomposition rate of ppb-level toluene by photocatalytic oxidation, Appl. Catal. B-Environ. 132–133 (2013) 212–218.

[31] A.H. Mamaghani, F. Haghighat, C. Lee, Photocatalytic degradation of VOCs on various commercial titanium dioxides: Impact of operating parameters on removal efficiency and by-products generation, Build. Environ. 138 (2018) 275–282.

[32] A.H. Mamaghani, F. Haghighat, C. Lee, Photocatalytic oxidation of MEK over hierarchical TiO$_2$ catalysts: Effect of photocatalyst features and operating conditions, Appl. Catal. B-Environ. 251 (2019) 1–16.

[33] H.E. Whyte, C. Raillard, A. Subrenat, V. Héquet, Photocatalytic oxidation of isoflurane, an anesthetic gas: the influence of operating parameters, Chem. Eng. J. 352 (2018) 441–449.